Exam III: A Comparison of Finite Element Analysis with Traditional Methods

Seth Berryhill

I Problem Statement

In this report results from two different methods for experimentally determining the stress concentration factor for a given notched beam are being compared. The first method is analytic, using equations derived from experimental data, while the second method is numeric, using the finite element analysis program Abaqus.

Geometry and Dimensions

The geometry of the piece investigated in the report is as shown in Figure 1.
The notches referred to in this report are specifically u-notches where a rounded edge is applied to a large rectangular notch. The stress concentration factor for a u-notched beam is a function of the geometry of the loaded beam and the notch. The height, H, of the beam is constant at 8.5 inches for all beams in this report. Other dimensions kept constant are t and d, which were 3.5 inches and 5 inches respectively.

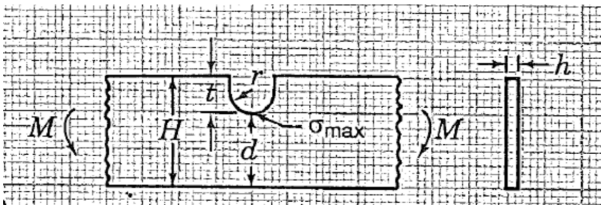

Figure 1: Beam geometry and loading.

The radius of the notches, r, is changed for each beam to show how different geometries effect the stress concentration factor.

Essential and Natural Boundary Conditions

The models tested were all split down a vertical axis of symmetry along the notch. Because of this the leftmost edge of the model, only including the vertical axis and not the inside edge of the notch, was fixed in the horizontal direction in order to recreate the opposing forces on the unmodelled half of the beam. This boundary condition does not restrict the natural movement of the beam as its centerline does not deform horizontally when subject to a symmetrical pair of forces or moments.

The second boundary condition applied to the model is a single point locked in the vertical axis. The bottom left corner of the model is chosen because it is not an edge or face subjected to this condition so the remainder of the model is free to deform around that point and the natural stress flow of the beam isn't interrupted in any way. This can be seen in Figure 3 on the next page.

Material Selection and Properties

Because the material properties do not effect the ratios of stress in the beam Nickel was chosen. Nickel has a Young's Modulus of $30,000$ ksi, and Poisson's ratio is 0.31 [1].

II Finite Element Model

Meshing the Model

The FEA models presented are all meshed using structured, quad-dominant meshes. Because the student version of the program limits models to less than 1000 nodes the mesh is less fine than optimal. Care was taken to make the mesh finer near the areas of interest, and very uniform in the general body of the part. This can be seen in Figure 2.

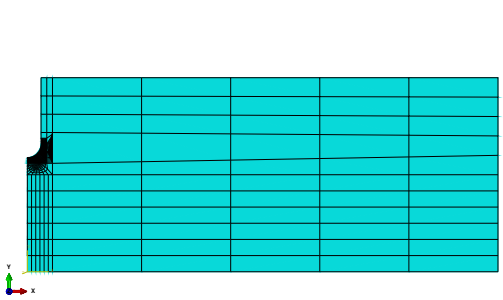

(a) An overview of the total mesh of the part. All models used the same mesh dimensions, and so got similar results.

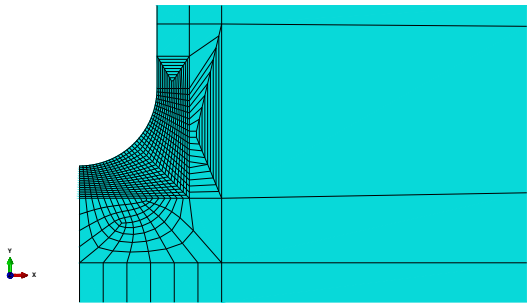

(b) A detailed view of finer meshes near the area of interest. To obtain more accurate results the nodes are placed more closely together near the notch's edge.

Figure 2

Loading the Model

The load being applied to the model is a pure bending moment, but unfortunately Abaqus doesn't support moment loading in 2-dimensional models. Due to this fact the load applied to the model is a distributed pressure, where the force at each point is equal to the applied moment multiplied by the distance from the point where the load is being applied. This can be seen in Figure 3 on the next page.

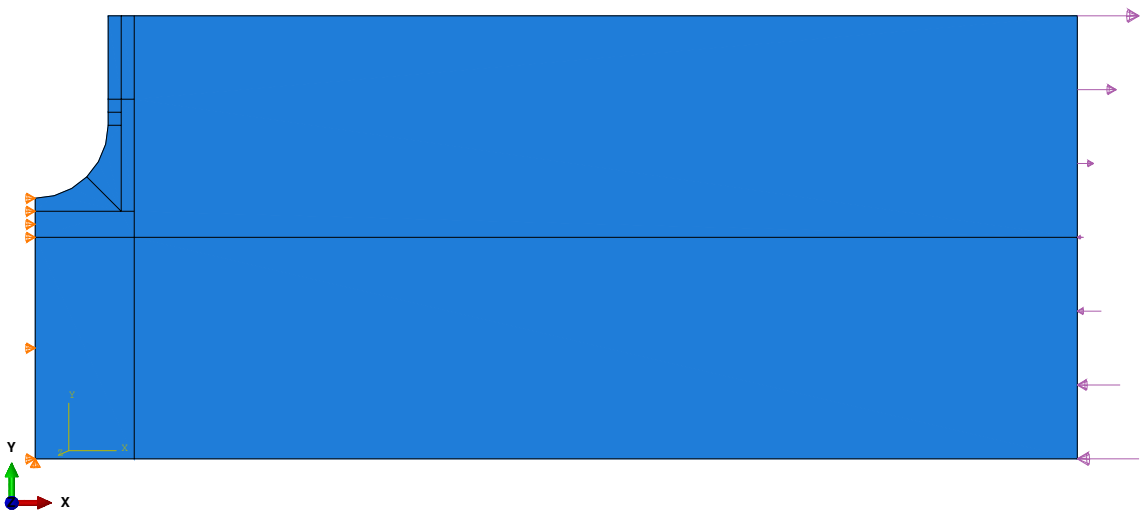

Figure 3: The boundary conditions of the model. On the left the fixed locations can be seen holding the part in place while the distributed pressure load can be seen on the right.

III Analytical Model

Equations

Experimental data was derived from photoelastic stress measurements [2]. From this data equations (1) - (9) were regressed. Photoelasticity is the phenomenon whereby clear, non-crystalline materials, such as plastics, will transmit light differently based on the stress state at each location in the material. This allows researchers to measure relative stress states based on the color of the light [3].

$$K_{tn} = C_1 + C_2\left(\frac{t}{H}\right) + C_3\left(\frac{t}{H}\right)^2 + C_4\left(\frac{t}{H}\right)^3 \tag{1}$$

For $\frac{t}{r}$ between 0.5 and 2 the $C_1 - C_4$ are:

$$c_1 = 1.795 + 1.481\left(\frac{t}{r}\right) - 0.211\left(\frac{t}{r}\right)^2 \tag{2}$$

$$c_2 = -3.544 - 3.677\left(\frac{t}{r}\right) + 0.578\left(\frac{t}{r}\right)^2 \tag{3}$$

$$c_3 = 5.459 + 3.691\left(\frac{t}{r}\right) - 0.565\left(\frac{t}{r}\right)^2 \tag{4}$$

$$c_4 = -2.678 - 1.531\left(\frac{t}{r}\right) + 0.205\left(\frac{t}{r}\right)^2 \tag{5}$$

And for $\frac{t}{r}$ between 2 and 20 the $C_1 - C_4$ are:

$$c_1 = 2.966 + 0.502\left(\frac{t}{r}\right) - 0.009\left(\frac{t}{r}\right)^2 \tag{6}$$

$$c_2 = -6.475 - 1.126\left(\frac{t}{r}\right) + 0.019\left(\frac{t}{r}\right)^2 \tag{7}$$

$$c_3 = 8.023 + 1.253\left(\frac{t}{r}\right) - 0.020\left(\frac{t}{r}\right)^2 \tag{8}$$

$$c_4 = -3.572 - 0.634\left(\frac{t}{r}\right) + 0.010\left(\frac{t}{r}\right)^2 \tag{9}$$

Code

Because these equations are cumbersome it is simpler to instead instantiate them using a computer programming language. This is an example of how one might write the equations in Python, an open source language, and create a graph of your outputs.

```
#Include libraries
import matplotlib.pyplot as plt #plotting software
import numpy as np #array handling library

#Initialize Variables
k = [] #Array of K values
rod = [] #Array of r/d values
t = 0.7 #Make sure H/d = 1.7
d = 1
H = t + d

# Create an array of values for r
```

```
increment = 0.001
r = np.arange(0.03,0.3, increment)

#increment through all values of r to find k
for i in range(0,len(r)):
    tor = t / r[i]
    toH = t / H

    if tor < 2:
        c1 = 1.795 + 1.481*tor - 0.211*tor**2
        c2 =-3.544 - 3.677*tor + 0.578*tor**2
        c3 = 5.459 + 3.691*tor - 0.565*tor**2
        c4 =-2.678 - 1.531*tor + 0.205*tor**2
    else:
        c1 = 2.966 + 0.502*tor - 0.009*tor**2
        c2 =-6.475 - 1.126*tor + 0.019*tor**2
        c3 = 8.023 + 1.253*tor - 0.020*tor**2
        c4 =-3.572 - 0.634*tor + 0.010*tor**2
    #Append this value of k to the array to make a full list
    k.append(c1 + c2*toH + c3*toH**2 + c4*toH**3)
    #Create array of r/d values
    rod.append(r[i]/d)
plt.plot(rod, k)#Plot Results
```

IV Results

Comparison of FEA and Analytical Models

The stress concentration of the FEA results are calculated with equations (10) and (11), where M represents the applied moment and h and d represent the height and depth of the beam respectively as seen in Figure 1 on page 1.

$$K_{tn} = \frac{\sigma_{max}}{\sigma_{nom}} \tag{10}$$

$$\sigma_{nom} = \frac{6M}{hd^2} \tag{11}$$

While the exact calculations can be found in appendix A this results in stress concentrations of 2.4, 1.9, and 1.7 for $\frac{r}{d}$ values of 1.2, 2.0, and 2.8 respectively. When compared to the analytical results this is an average error of 7.3%. These results are shown in Figure 4 on the next page.

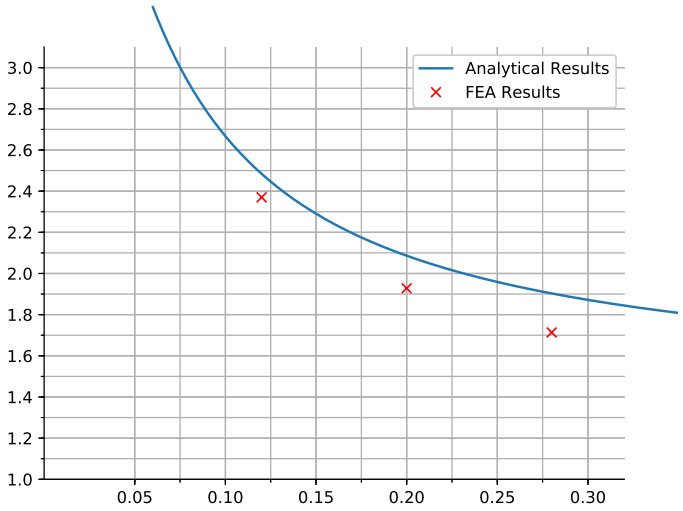

Figure 4: Comparison of FEA and analytical methods.

Discussion

The relatively low error between the analytical and numerical methods would seem to represent the ability of finite element analysis to accurately model the stress concentration in u-notched beam geometries. These results also match the provided graph of experimental data. Improvements to the model, such as more exact meshing and a larger cap on the number of mesh nodes would likely increase the accuracy of the model overall. Uncertainty in the experimental data used to construct the analytical model is not available at the moment, and so it is also not possible to perform a statistical analysis of the results. If the deviation of experimental results was large then it is possible that the FEA results are more exact than the regressed equations.

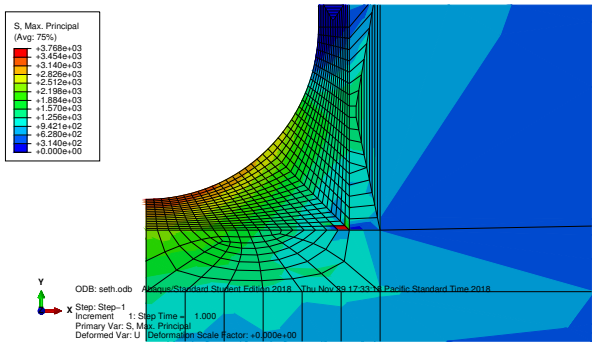

Figure 5: An example of FEA results. This image shows the stress flow of a notch with an 1800 in-lb moment applied to the end of the beam. The model only represents one half of the axis of symmetry to reduce computational demand.

A Appendix

r/d	M (in-lbf)	σ_{max} (psi)	σ_{nom} (psi)	k_{fea}	k_{eqn}	error%
1.2	8500	4834.69	2040	2.3699	2.4839	-4.6
2.0	8500	3933.23	2040	1.9281	2.0862	-7.6
2.8	8500	3495.53	2040	1.7135	1.9029	-9.9

List of Figures

References

[1] J. B. Miner, D. & Seastone, *Handbook of Engineering Materials*, ser. Wiley engineering handbook series. New York; Chapman & Hall: London, 1955.

[2] G. Potirniche, "Me 341 - exam 3 - take home," 2018, exam Handout.

[3] W.-C. Wang. (2018) Photoelasticity. [Online]. Available: https://depts.washington.edu/mictech/optics/me557/photoelasticity.pdf